Scientific Paper

Nanodesigning of SiO_2: Eu^{3+} Particles Obtained by Spray Pyrolysis Method and Their Luminescence Properties†

Vukoman Jokanović, Miroslav D. Dramićanin,* and Željka Andrić

Institute of Nuclear Sciences "Vinča," P.O. Box 522, 11001 Belgrade, Serbia and Montenegro.
E-mail: dramican@vin.bg.ac.yu

Received 08-04-2005

†Paper based on a presentation at the 14th International Symposium "Spectroscopy in Theory and Practice", Nova Gorica, Slovenia, 2005.

Abstract

Mechanism of droplet formation and the structuring of SiO_2:Eu^{3+} spheres prepared by the process of ultrasonic spray pyrolysis, using colloidal solution consisting of the 7.5 nm SiO_2 nanoparticles and $Eu(NO_3)_3 \cdot 6H_2O$ as a precursor, is described. The proposed model quantitatively defines each line in the size distribution spectrum. Agreement between theoretically obtained basic structural parameters (size distribution and geometry) and experimentally determined values was found. Electron microscopy of SiO_2:Eu^{3+} powder revealed three-level arrangement of material: nanoparticles, sub-particles and spheres, also in agreement with the theoretical model. Luminescence properties of trivalent europium ions imbedded in such structured system are investigated in addition. Characteristic emissions of $^5D_0 \rightarrow {}^7F_J$ transitions of Eu^{3+} ion were found with a good chromaticity and very good luminescence lifetime of 3.3 ms.

Key words: spray pyrolysis, nanodesigning, silica sol, europium, luminescence.

Introduction

Silica can be used as an insulation material in integrated circuits, due to a low dielectric constant. Such ceramics has unique optical properties which are used in the production of optical filters, because its reflectivity and transmission depend strongly on the wavelength. It is also a candidate for the photon band gap materials.[1–3]

Due to good optical transmittance, mechanical hardness, chemical durability, thermal stability, low temperature expansion coefficient, and high laser damage threshold, the high performance silicon dioxide ceramics and glass based on it, are extensively applied as optoelectronic laser diodes, telecommunication optical fibres, medical laser delivery systems and military optical sensors.[4]

The spray pyrolysis uses well defined precursors such as silicon dioxide sol synthesized in autoclave as a nanostructure's material with a well defined structure; particles form and their distribution, at both particle and sub-particle levels.[5–10] It enables maintenance of the structure generated in the precursor throughout the spray pyrolysis process all resulting in a highly active structure suitable for different applications of silicon dioxide we have mentioned here.

The obtained silicon dioxide particles are suitable for designing of the self-assembling films with a high and well defined porosity, for example by very slow precipitation of particles at the substrate surface as described in a recent review.[10] The particles can also be carriers of active ionic types such as rare earth or other elements for highly selective applications in optics and electronics.

Results and discussion

Arrangement of basic particles in the powder obtained after spray pyrolysis has been investigated by transmission electron microscopy (TEM) and scanning electron microscopy (SEM).

The particle size of silica sol used as a precursor for obtaining SiO_2 powder was determined TEM. The microphotograph in Figure 1 shows that silica particles have a size between 5 and 10 nm, while their shape is mostly spherical representing agglomerates of finer particles. The mean particle size is 7.5 nm.

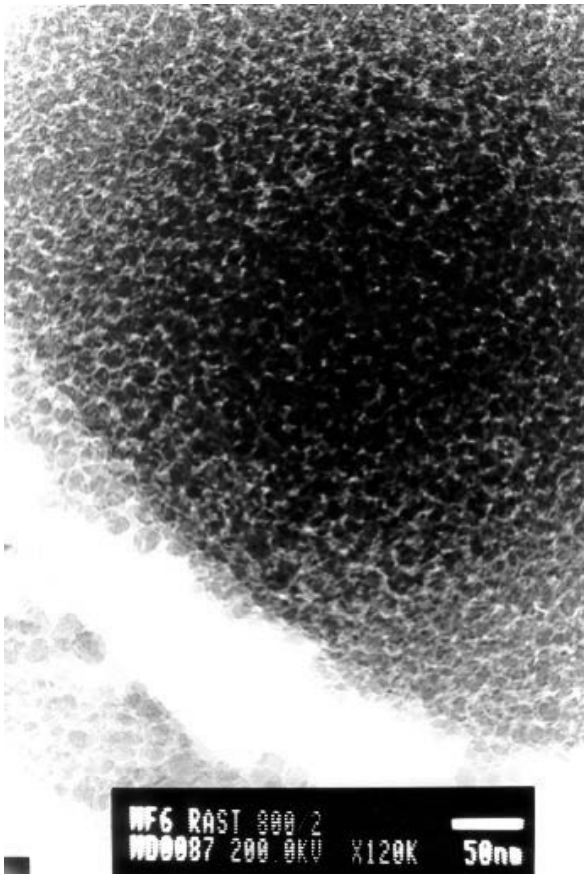

Figure 1. Size and morphology of the silica sol particles.

Networking of sol particles in the primary sub-particles, and then in the secondary SiO_2 particle structure (particle structure as a whole) was experimentally determined. Typical distribution of SiO_2 particles is presented in Figure 2 and Table 1.

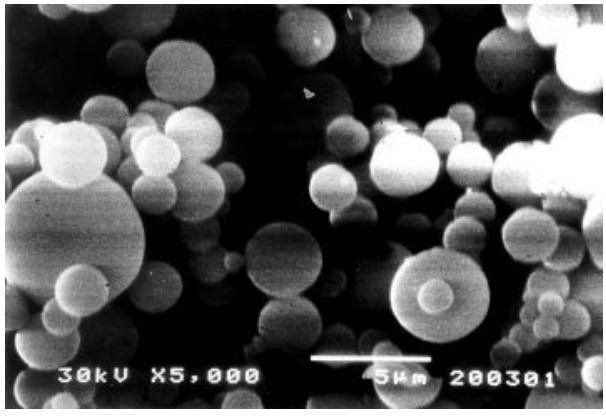

Figure 2. Typical distribution of SiO_2 particles obtained by the spray pyrolysis.

Table 1. Experimentally obtained distribution of secondary SiO_2 particles, d_p.

d_p [μm]	1	1.25	1.5	1.75	2.5	3.5
Relative frequency of occurrence [%]	4	19	35	27	12	3

The mean diameter of the secondary SiO_2 particle, d_{ap}, is obtained from the following equation:

$$d_{ap} = \sum_{i=1}^{N} n_i d_i \Big/ \sum_{i=1}^{N} n_i ,$$

where n_i represents number and d_i the diameter of particles in a i^{th} class interval, respectively, and N stands for the total number of distribution intervals. According to this equation we find the mean diameter of the secondary SiO_2 particle to be 1.68 μm.

Theoretical model, given in brief in Appendix A1, allows calculations of the discrete droplet and particle size distributions of the investigated powder. Similar calculations have been successfully employed and experimentally validated for various systems[5,6,11–17] (TiO_2, Al_2O_3, mullite, calcium hydroxyapattite, etc). The other theoretical models, like Peskin and Raco model and Lange equation, give only the mean particle diameter. Comparison of these models to the one applied here has been discussed in detail in Ref. 10. Based on this model the aerosol droplet diameters are calculated by using the appropriate equations (Appendix A1, Equation A4 and Equation A5) and found to be between 3.6 μm and 7.5 μm having average diameter of 4.14 μm. In the next step of calculations the discrete values for the particle diameter were obtained by applying equation for volume reduction factor, which defines the decreasing of particle size during solidification stage of the synthesis process consisted from precipitation, drying and thermo-pyrolysis (Appendix A2, Equation A5). These values are within the interval 1.22 μm to 2.55 μm. The average SiO_2 particle diameter estimated by the employed theoretical model has the value of 1.83 μm, which agrees reasonable good with the experimentally obtained value of 1.68 μm. If we look at the discrete values for diameters in the theoretical particles sizes distribution obtained (Table 2) by using Equation A6 and Equation A7, given in Appendix A1, and compare them with the distribution of experimentally measured particles diameters, it can be elucidated that in both cases distributions are narrow, within approximately the same interval.

Table 2. Calculated distribution of SiO_2 particles, d_p.

d_p [μm]	1.22	1.89	2.55
Relative frequency of occurrence [%]	32	45	23

One may notice on Figure 3 that each particle has a complex substructure, which shows that inside a particle there are numerous sub particles. From the microscopy data obtained with larger magnifications (not show here) we assessed the diameters of these sub-particles from 25 to 30 nm.

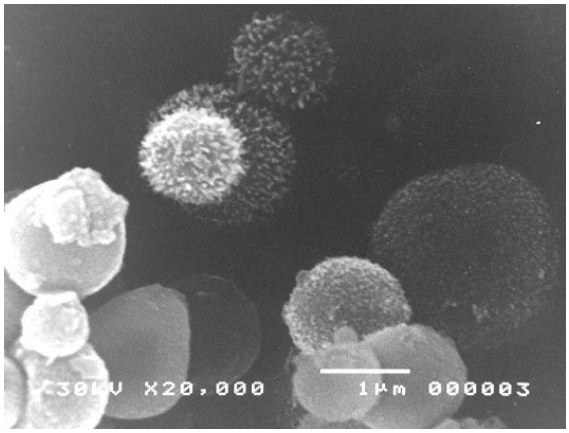

Figure 3. A typical sub-structure of SiO_2 particles obtained by spray pyrolysis.

Taking into account theoretical model related to the substructure particles designing, Appendix A2, the average sub-droplet and sub particle size (d_{sd}) were calculated using Equation A10 given in Appendix A2 and Equation A5 in Appendix A1. These values are found to be d_{sd} = 128 nm and d_{sp} = 38.4 nm, respectively.

Based on above results one can conclude that the synthesized system is composed of the three-structure levels: basic or secondary particles with a mean diameter of 1.8 μm, primary or sub-particles with a mean diameter of 38.4 nm; and the sol particles 5–10 nm in size that form the sub-particles.

Luminescence properties: Room temperature phosphorescence emission spectra, excited at 393 nm, of the SiO_2:Eu^{3+} powder obtained by spray pyrolysis is presented on Figure 4.

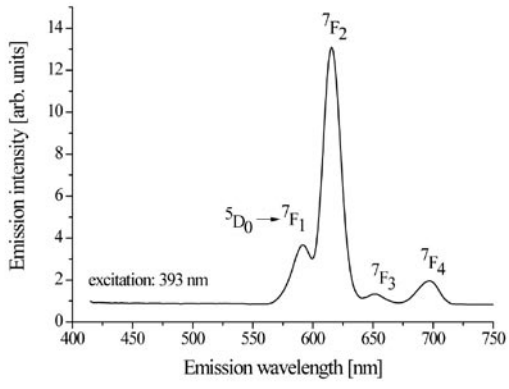

Figure 4. Phosphorescence emission spectrum of SiO_2:Eu^{3+} powder.

Upon excitation europium doped silica powders exhibit strong red phosphorescence. The emission bands correspond to the intraconfigurational $^5D_0 \rightarrow ^7F_J$ (J = 1, 2, 3, 4) spin forbidden f-f transitions of the Eu^{3+} ion.[18] The $^5D_0 \rightarrow ^7F_1$ transition band at 590 nm is the parity-allowed magnetic dipole transition (ΔJ = 1) and its intensity does not vary with the host. On the contrary, the $^5D_0 \rightarrow ^7F_2$ electric dipole transition band at 616 nm (ΔJ = 2) is very sensitive to the local environment around Eu^{3+}, and its intensity depends on the symmetry of the crystal field around the europium ion. A low symmetry around the rare earth cation increases the emission strength of the electric dipole transition. In this sense, it is generally admitted that the ratio of the emission intensities R = I ($^5D_0 \rightarrow ^7F_2$) / I ($^5D_0 \rightarrow ^7F_1$) is an asymmetry parameter for the Eu^{3+} sites and a measure of the extent of its interaction with surrounding ligands. This asymmetry parameter is often called chromaticity index since it represents the ratio of the red emission intensity over the orange. The chromaticity index value of 3.59 is derived from the Figure 4. In addition, well resolved emission bands at 650 nm and 700 nm that originate from $^5D_0 \rightarrow ^7F_3$ and $^5D_0 \rightarrow ^7F_4$ transitions can be indubitably identified on the spectrum.

One can clearly observe red shift of $^5D_0 \rightarrow ^7F_J$ phosphorescence emissions. This happens because of two reasons. First, phosphorescence emission occurs at longer wavelength than fluorescence due to slight loss in energy during fast transition from singlet to triplet state, the transition that precedes phosphorescence deexcitation. Second, the red shift is also consequence of a very small grain size of investigated material. Trivalent europium ions are imbedded in nanoparticles, the basic elements of sub-particles and spheres formed during the spray pyrolysis process. Nanoparticle properties differ from those of conventional materials influenced by the particle size.[19–22] Although the electronic states of rare earth ions are quite localized to dimensions of much smaller than the size of nanoparticle, the structure of nanoparticles is not necessarily equal to that of the bulk and therefore nanoparticles may have very different spectra then bulk material. Also, because of their proximity to the boundary of the nanoparticle the rare earth ions may interact with defects at the surface or with the medium in which they are imbedded altering their linewidths.[23]

Although vibrations of residual hydroxyl groups and water near Eu^{3+} ions may provide a nonradiative decay mechanism for the Eu^{3+}, luminescence lifetime measurement, shown on Figure 5, reveals long luminescence intensity decay of Eu^{3+} doped silica nanopowder. The measurement is performed for the $^5D_0 \rightarrow ^7F_2$ transition. The deviation from the straight line at short measurements times indicate complex deexcitation path in the investigated sample. The

luminescence lifetime τ_{long}, calculated for higher measurement times from the part of decay curve that has a linear slope, is 3.3 ms, a quite high value characteristic of europium species with low non-radiative energy transfer probability.

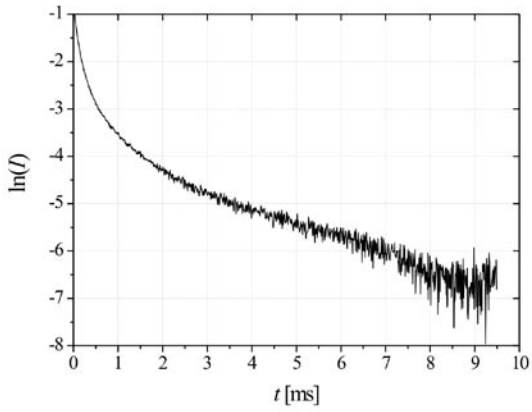

Figure 5. Luminescence decay measurement for the $^5D_0 \rightarrow ^7F_2$ transition in Eu^{3+} doped silica powders.

Conclusions

In this paper the synthesis mechanism of silicon dioxide particles obtained using spray pyrolysis by spraying mixture of silica sol and Eu^{3+} as a precursor has been presented. The structural design of the particles obtained at different levels starting with the particle as a whole, via sub-particles participating in the formation of these particles to silica sol particles was defined.

According to SEM and TEM measurements the mean particle size after spray pyrolysis was 1.68 μm, sub- particle size was 25–30 nm, while corresponding calculated values, obtained on the basis of presented model, were 1.8 μm and 38.4 nm, respectively. The average diameter of sol particles is found to be from 5 to 10 nm (TEM). Calculations based on presented theoretical model show reasonable agreement with the experimental results obtained both on powder particle level and sub-particle levels and confirm applicability of model to investigated system and also for the structural design of similar systems.

Luminescence spectroscopy measurements clearly show characteristic emissions of Eu^{3+} ion. The material has good chromaticity and very good luminescence lifetime. Because of that it is our opinion that this material has a very good potential for luminescence based applications.

Experimental

Sol and powder preparation: The silica sol was prepared by soaking water glass solution ($Na_2O \times 3SiO_2$ with silicate module SiO_2/Na_2O ratio of 3.75 in de-ionized water) viscosity of 2.2 Poas, with 0.1M HCl solution. Soaking was accomplished by dripping the 0.1M HCl solution; drop by drop, into a pot containing the water glass solution intensively mixed with a magnetic mixer. The mixing temperature was 80 °C.

After addition of the total amount of 0.1M HCl required for complete neutralization of water glass the whole system was transferred into an autoclave, and the soaking was continued for 5 h at the temperature of 120 °C and pressure of 3 bars.

The obtained silicon acid precipitate was then separated from the solution using an ultracentrifuge with 10.000 rotations per minute followed by an extra addition of de-ionized water in order to set the liquid/solid phase ratio on 4:1.

In the second phase of the preparation procedure the silicon acid precipitate was transformed into sol. It was achieved by taking 20 g of silicon acid obtained by soaking, using the outlined procedure, and than 200 mL of deionised water, which pH was set to 10 (using 0.1N NaOH solution) was added. The system was then intensively mixed again at 80 °C for a further 2 hours, and its pH was set again on 10 by dripping in the 0.1M NaOH solution. The content was than transferred into an autoclave and treated further at 120 °C and pressure of 3 bars for 8 h. Upon completion of hydrothermal treatment, the pH of the silicon acid sol was 9. The concentration of obtained sol solution was set to the value of 2M of silica.

Finally, 3 at% Eu^{3+} as europium nitrate were added to silica sol to obtain a precursor for ultrasonic spray pyrolysis.

The pyrolysis conditions were as following: the frequency of the ultrasonic atomizer was 1.7 MHz, working temperature in the tubular furnace was 1000 °C and the carrier gas-air-flow rate was 0.011 m/s.

Characterization methods: The following methods were used in the characterization of synthesized materials: transmission electron microscopy - TEM (JOEL JEM 2000 FX). The morphology, size distribution, the mean size of silicon dioxide particles, and substructure were determined using scanning electron microscopy - SEM (JEOL: JKSM-5300). The samples for SEM were prepared by coating of powder with the gold, using the PVD method.

Room temperature luminescence and phosphorescence of SiO_2:Eu^{3+} nanopowders have been measured on Perkin Elmer LS45 luminescence spectrometer. For phosphorescence measurements the instrument was setting in an appropriate mode with 0.5 ms delay time (delay from beginning of excitation pulse to beginning of observation) and 0.1 ms gate time (the gate width of detector). Luminescence lifetime measurements were made using NT340 Series

EKSPLA OPO (Optical Parametric Oscillator) for the sample excitation at 460 nm (pulse duration of 5.2 ns) and oscilloscope for the data collection from photomultiplier tube.

Acknowledgements

This work was supported by the Serbian Ministry of Science and Environment Protection.

Appendix A1: *Theoretical model describing structure designing of secondary particles by ultrasound spray pyrolysis.*

Waves that form by transferring ultrasound oscillations in a given precursor, depending on the superposition conditions have a complex spatial form that primarily depends on oscillation muting factors in different directions (in the direction of deformation or in the direction perpendicular to it) and the compulsory frequency of the ultrasonic generator.[5–10] For small enough thicknesses of the liquid column the difference in the muting factor of transversal and longitudinal waves is insignificant, so in this case in the process of compulsory ultrasound excitation standing waves with a spherical form are obtained.[5–10] Based on a 3D model of capillary standing waves formed at a meniscus surface the following expression is obtained by analyzing the harmonic potential rate function of the disruption formed:[5–10]

$$\frac{\partial \varphi}{\partial t} + g\xi - \frac{\sigma}{\rho}\left[\frac{\partial^2 \xi}{\partial x^2} + \frac{\partial^2 \xi}{\partial z^2}\right] = 0, \qquad \text{(A1)}$$

where ϕ is the potential rate of capillary standing waves, σ is the surface solution tension, g is the inertial force acting on the liquid in contact with the ultrasonic oscillator, ξ is the amplitude of the standing wave formed, x and z are coordinates equivalent to the given amplitude and t is the time.

The final solution of equation (A1) can be written in the following form:[5–10]

$$d = \left(\frac{\pi\sigma}{\rho f^2}\right)^{\frac{1}{3}}, \qquad \text{(A2)}$$

where d represents the mean radius of the aerosol droplet formed, ρ is the solution density and f is the excitation frequency of the given ultrasonic oscillator.

If it is assumed that the difference in the muting factor of transversal and longitudinal waves is not insignificant, as the thickness of the liquid column is not insignificant then it is possible to present the standing capillary wave in the form of a Laplace equation expressed in polar coordinates:[5–10]

$$\rho\frac{\partial^2 \varphi}{\partial t^2}_{r=R} - \frac{\sigma}{R^2}\left\{2\frac{\partial \varphi}{\partial r} + \frac{\partial}{\partial r}\left[\frac{1}{\sin\theta}\frac{\partial\left(\sin\theta\frac{\partial \varphi}{\partial \theta}\right)}{\partial \theta} + \frac{1}{\sin^2\theta}\frac{\partial^2 \varphi}{\partial \varepsilon^2}\right]\right\} = 0, \qquad \text{(A3)}$$

where r is the aerosol droplet radius, ε and θ are angles corresponding to the equation transformed into polar coordinates.

The solution of this equation gives a set of solutions corresponding to possible discrete values of aerosol droplet radiuses, equivalent to the given muting factor of excited capillary waves in a given liquid column:

$$D = \frac{1}{\pi}\left(\frac{2\sigma\pi}{\rho f^2}\right)^{\frac{1}{3}}\left[l(l-1)(l+2)\right]^{\frac{1}{3}}, \qquad \text{(A4)}$$

Finally, in order to obtain diameter values for particles forming from aerosol droplet diameter values through the solidification process of aerosol droplets the following equation is used equation:[5–10]

$$d_p = d_d\left(\frac{c_{pr}M_p}{\rho_p M_{pr}}\right)^{\frac{1}{3}}, \qquad \text{(A5)}$$

where d_p is the powder particle diameter, ρ_p is the powder density, M_p is the molecular mass of the powder, c_{pr} is the precursor concentration (solution used for spraying when obtaining powder particles) and M_{pr} is the molecular mass of the precursor.

The particle size distribution can be estimated from the equation:[5–10]

$$I_1 : I_2 : \ldots : I_N = \frac{1}{\Delta f_1} : \frac{1}{\Delta f_2} : \ldots : \frac{1}{\Delta f_N} \qquad \text{(A6)}$$

where I_1, I_2, I_N are frequencies of occurrence of corresponding discrete values of particle diameters in a given spectra, while Δf_1, Δf_2,…,Δf_N are displacements of the real frequencies from the forced frequency of the ultrasonic oscillator caused by damping factor of the precursor liquid column. The relative ratios of intensity-the frequency of a particular diameter-if normalized provides the basic relationship for calculation of the absolute value for the occurrence frequency:[5–10]

$$I_1 + I_2 + \ldots + I_N = 1 \qquad \text{(A7)}$$

Appendix A2: *Theoretical modelling of the powder particle sub-structure.*

The radius of nanoelements/nanodroplets and nanoparticles forming the given aerosol droplet substructure, i.e. the secondary particles that forms by its solidification can be determined using the wave equation of a centrally symmetric standing wave formed as the result of transferred excitation of the ultrasonic generator to the droplet itself that can be described as:[7–9]

$$\frac{\partial^2 \varphi}{\partial t^2} = c^2 \frac{1}{r^2} \frac{\partial}{\partial r}\left(r^2 \frac{\partial \varphi}{\partial r} \right), \qquad \text{(A8)}$$

where c is the disturbance-spreading rate and r is the aerosol droplet radius.

Based on the derivation[7–9] the following equation solution is obtained:

$$\tan(kr) = kr, \qquad \text{(A9)}$$

where k is the wave number ($k = \frac{2\pi f}{c}$) whose numerical solution is given by the set:[7–9]

$$r = \frac{\Psi c}{f}, \qquad \text{(A10)}$$

where Ψ is a numerical constant that has different values for different solutions (values of the numerical constant as a set of solutions of equation (A5) are given as 0.175, 1.21, 1.72, 2.23, 2.74, 3.82,... and they depend on the form of sub-structural elements comprising the particle formed in the droplet - aerosol sub-droplet solidification process.

References

1. R. Reisfeld, *Mat. Sci*. **2002**, *20*, 5–18.
2. M. Morita, D. Rau, S. Kajyama, T. Sakurai, M. Baba, M. Iwamura, *Mat.Sci.-Poland* **2004**, *22*, 5–15.
3. A. N. Trukhin, M. Goldberg, J. Jansons, H.-J. Fitting, I. A. Tale, *J. Non-Cryst. Solids* **1998**, *223*, 114–122.
4. O. D. Velev, T. A. Jede, R. F. Lobo, A. M. Lenhoff, *Nature*, **1997**, *389*, 447–448.
5. V. Jokanović, Dj. Janaćković, A. M. Spasić, D. Uskoković, *Mater. Trans. JIM* **1996**, *37*, 627–635.
6. V. Jokanović, Dj. Janaćković, D. Uskoković, *Ultrason. Sonochem.* **1999**, *6*, 157–169.
7. A. Kulak, S. A. Davis, E. Dujarin, S. Mann, *Chem. Mater.* **2003**, *15*, 528–535.
8. V. Jokanović, A. M. Spasić, D. Uskoković, *J. Coll. Interf. Sci.* **2004**, *278*, 342–352.
9. G. V. Jayanthi, S. C. Zhang, G. L. Messing, *J. Aerosol Sci. Technol*. **1993**, *19*, 478–490.
10. V. Jokanović In *Finely Dispresed Particles: Micro, Nano, and Atto-engineering*; A. Spasić, J. P. Hsu, Eds.; CRC Press: New York, 2005, Chapter 20.
11. Z. V. Šaponjić, Z. Rakočević, N. M. Dimitrijević, J. M. Nedeljković, V. Jokanović, D. P. Uskoković, *Nanostruct. Mater*. **1998**, *10*, 333–339.
12. J. Nedeljković, Z. Šaponjić, Z. Rakočević, V. Jokanović, D. Uskoković, *Nanostruct. Mater*. **1997**, *9*, 125–128.
13. V. Jokanović, Dj. Janaćković, A. M. Spasić, D. Uskoković, *Mat. Trans. JIM* **1996**, 37, *4*, 627–634.
14. V. Jokanović, Dj. Janaćković, P. Spasić, D. Uskoković, *Nanostruct. Mater*. **1999**, *12*, 349–352.
15. V. Jokanović, Dj. Janaćković, R. Ćurčić, P. Živanović, D. Uskoković, Materials Science Forum **1998**, *282–283*, 65–70.
16. V. Jokanović, Dj. Janaćković, D. Uskoković, *Key Engin. Mater*. **1997**, *132–136*, 197–200.
17. Dj. Janaćković, I. Petrović-Prelević, Lj. Kostić-Gvozdenović, R. Petrović, V. Jokanović, D. Uskoković, *Key Eng. Mater*. **2001**, *13*, 192–195.
18. G. Liu In *Spectroscopic Properties of Rare Earths in Optical Materials*; G. Liu, B. Jacquier, Eds.; Springer: Berlin Heidelberg, 2005; Chapter 1.
19. A. J. Kenyonn, C. E. Chryssou, C. W. Pitt, *J. Appl. Phys.* **2002**, *91*, 367–374.
20. A. Konrad, T. Fries, A. Gahn, *J. Appl. Phys.* **1999**, *86*, 3129–3133.
21. G. Tessarli, M. Bettinelli, A. Speghini, *Appl. Surf. Sci.* **1999**, *144–145*, 686–689.
22. W. Y. Jia, Y. Y. Wang, F. Fernandez, *Mater. Sci. Eng. C* **2001**, *16*, 55–58.
23. R. S. Meltzer In *Spectroscopic Properties of Rare Earths in Optical Materials*; G. Liu, B. Jacquier, Eds.; Springer: Berlin Heidelberg, 2005; Chapter 4.

Povzetek

Opisan je mehanizem tvorbe kapljic in strukturiranja SiO_2:Eu^{3+} sferičnih delcev, pripravljenih s postopkom pirolize z ultrazvočnim naprševanjem iz koloidne raztopine nanodelcev SiO_2 (velikosti 7.5 nm) in $Eu(NO_3)_3 \cdot 6H_2O$ prekurzorja. Predlagani model kvantitativno določa vsako črto v porazdelitvenem spektru velikosti delcev. Teoretični osnovni strukturni parametri (porazdelitev velikosti in geometrija) in eksperimentalne vrednosti se ujemajo. Elektronska mikroskopija prahov SiO_2:Eu^{3+} je skladno s teoretičnim modelom razkrila tri nivoje organiziranosti materiala: nanodelce, poddelce in sferične delce. Raziskali smo tudi luminiscenčne lastnosti trivalentnih evropijevih ionov v opisanih strukturah, ki se odražajo v značilnih emisijskih črtah za $^5D_0 \rightarrow {}^7F_J$ prehode z razpolovnim časom 3.3 ms.